

## Photochemistry of “Super” Photoacids. 2. Excited-State Proton Transfer in Methanol/Water Mixtures

Kyril M. Solntsev,<sup>\*,†,‡</sup> Dan Huppert,<sup>†</sup> Noam Agmon,<sup>‡</sup> and Laren M. Tolbert<sup>§</sup>

Raymond and Beverly Sackler Faculty of Exact Sciences, School of Chemistry, Tel Aviv University, Tel Aviv, 69978, Israel, Department of Physical Chemistry and Fritz Haber Research Center, The Hebrew University, Jerusalem, 91904, Israel, and School of Chemistry and Biochemistry, Georgia Institute of Technology, Atlanta, Georgia, 30332-0400

Received: December 23, 1999; In Final Form: March 6, 2000

Excited-state proton transfer to solvent (PTTS) of 5-cyano-2-naphthol was investigated in methanol/water mixtures. We have found that the time-resolved fluorescence data fit the solution of the Debye–Smoluchowski equation for the reversible geminate recombination of ions over the whole range of methanol/water concentration ratios. The rate constants of the elementary protolytic photochemical processes and their isotope effects were determined by a simultaneous analysis of the time-resolved fluorescence of the photoacid and its conjugated anion. The competition between adiabatic protonation and quenching of the excited naphtholate anion by the geminate proton was observed to diminish sharply near pure methanol. The dissociation rate coefficient near pure methanol depends on a power of the water concentration, which appears to decrease from 2 (for “ordinary” photoacids) to below 1 for “super” photoacids.

### I. Introduction

Proton transfer, in both ground and excited states, is a fundamental process in chemistry and biology. The subject of our current research is the investigation of the mechanism of ultrafast excited-state proton transfer reactions of exceptionally strong photoacids in methanol/water solutions. Protolytic photodissociation (excited-state proton transfer to solvent or PTTS) has been studied intensively in the past 50 years.<sup>1</sup> The acidity of various hydroxyaromatic compounds (ROH) increases significantly upon excitation, and therefore molecules of this type are widely used as excited-state acid–base fluorescent probes in homogeneous solutions and microheterogeneous systems.

The influence of water structure on the PTTS kinetics is most conspicuous in the investigation of proton transfer in mixed water/organic solvents. Protolytic photodissociation of various hydroxyaromatic compounds was studied in series of mixtures of water with alcohols<sup>2–18</sup> and other solvents.<sup>14,19,20</sup> In all cases PTTS rates were found to decrease with decreasing molar fraction of water in the mixture. This was accompanied by an increase of excited ROH (R\*OH) fluorescence decay times and quantum yields, and a reduction of R\*O<sup>−</sup> emission. For 2-naphthol (2OH, pK<sub>a</sub><sup>\*</sup> = 2.8) the protolytic dissociation can be observed only up to 50 vol % methanol.<sup>7</sup> At higher methanol contents, the typical dissociation time becomes considerably longer than the excited-state lifetime (typically, 5–10 ns). For a much stronger photoacid like 1-naphthol (1OH, pK<sub>a</sub><sup>\*</sup> = 0.4), dissociation is still observed at 98 wt % MeOH.<sup>9</sup>

It was suggested<sup>5–7</sup> that a proton transfers only to water clusters of a certain size. In contrast to water solutions where such clusters already exist in the ROH solvation shell, in mixed solvents an additional step of their formation takes place.

Robinson et al.<sup>7</sup> described it as a sequence of reversible processes corresponding to the substitution of alcohol molecules in the ROH solvation shell with water. This sequence terminates when the cluster size reaches a critical value. Experimental PTTS rate constants in methanol/water mixtures of different compositions are in best agreement with this model at critical cluster size of 4 ± 1. This cluster size was identical for both fast (1OH) and slow (2OH) photoacids.<sup>14</sup>

Schulman et al.<sup>13,19</sup> studied PTTS of 2OH, 2,6-naphtholsulfonate, and 8-hydroxy-1,3,6-pyrenetrisulfonate (HPTS) in ethanol/water and DMSO/water mixtures. It was found that the overall dissociation rate constant, *k*<sub>off</sub>, had a linear dependence on the water activity, α(H<sub>2</sub>O), of the corresponding solution:

$$\ln(k_{\text{off}}\tau_0) = \ln(k_{\text{off}}^\circ\tau_0) + \rho \ln \alpha(\text{H}_2\text{O}) \quad (1)$$

where *k*<sub>off</sub><sup>°</sup> is the rate constant in pure water (α = 1) and τ<sub>0</sub> is the lifetime of the R\*OH in its lowest excited state in water in the absence of proton transfer. It was found for all compounds that ρ = 12, and this value was interpreted as the number of water molecules in the proton acceptor cluster.<sup>13,19</sup> The significant difference with the value of 4 ± 1 obtained by Robinson et al.<sup>5–7,14</sup> was explained by the possible involvement of water molecules of outer coordination shells in the reaction.

Klein et al.<sup>11c</sup> suggested that protolytic photodissociation of 1-hydroxy-4-naphthalenesulfonate (4S1OH) (pK<sub>a</sub><sup>\*</sup> ≈ −0.1 in water) in propanol/water mixtures requires a critical water concentration (4.1 ± 0.3 M at 25 °C). Above this critical value, only two water molecules are needed to sustain the proton-accepting cluster.

Agmon et al.<sup>9</sup> applied the theory of geminate diffusion-influenced reactions<sup>21</sup> to the PTTS of HPTS in methanol/water mixtures in the water-rich region. At all water concentrations the kinetics obeyed the transient Smoluchowski equation for diffusion of the geminate proton in a Coulomb potential with “back-reaction” boundary conditions. This was manifested in

\* Address correspondence to this author at The Hebrew University. E-mail: solntsev@fh.huji.ac.il.

† Tel Aviv University.

‡ The Hebrew University.

§ Georgia Institute of Technology.

the  $R^*OH$  fluorescence signal, which turned over from an initial exponential decay to a long-time power law ( $t^{-3/2}$ ). Thus kinetically water molecule diffusion, which is supposedly required to form the critical cluster, is not observed.<sup>9</sup>

In all cases described above the range of solvents investigated has been limited to water and its mixtures with various organic solvents for which the acidity of photoacids was sufficient to observe photodissociation:  $k_{off} \geq 0.1/\tau_0$ . Simple estimation using the well-known Brønsted-type correlations<sup>1d,17,22</sup> between  $\log k_{off}$  and  $pK_a^*$  on one hand and the known differences between acidity constants in water and in methanol<sup>23,24</sup> on the other, suggests that a photoacid capable of protolytic photodissociation in pure methanol must have  $pK_a^* \leq 0.5$  in water.

The influence of substituents on the acidity of hydroxyaromatic compounds is well described in the literature.<sup>25</sup> The cyano group is one of the strongest electron-withdrawing groups (Hammett substituent constant  $\sigma = 0.6-0.7^{25}$ ). Tolbert et al.<sup>26</sup> have synthesized several cyano-substituted naphthols [e.g., 5-cyano-2-naphthol (5CN2OH), 5,8-dicyano-2-naphthol (DCN2), and some others]. These compounds, being very strong photoacids ( $pK_a^* < 0$  in water), were found to transfer their proton not only to water, but also to solvents with lower polarity, such as alcohols, amides, and DMSO.<sup>18,26-28</sup> We have investigated PTTS from 5CN2OH to neat organic solvents in part 1 of this series.<sup>29</sup>

It was demonstrated that both ground- and excited-state  $pK_a$ 's are sensitive to the position of the substitution on the naphthalene ring.<sup>26,28,29</sup> It is known that electrophilic attack on naphthols in thermal organic reactions (such as the Friedel-Crafts acylation) is directed toward specific aromatic carbon atoms depending on the hydroxyl group location. For 1OH the attack is on positions C-2 and C-4 whereas for 2OH it is on C-1 and C-6.<sup>30</sup> Incorporation of an electron donor (or acceptor) substituent in these positions leads to a pronounced decrease (or, correspondingly, increase) in ground-state naphthol acidity.<sup>25,31</sup>

Upon excitation, the electron density of naphthols moves from the oxygen toward the distal ring, and therefore the target of an electrophilic attack changes as compared to the ground state. One of the most investigated excited-state electrophilic substitution reactions in naphthols is fluorescence quenching by protons.<sup>32</sup> Using IR and NMR methods it was shown that photochemical hydrogen/deuterium exchange on the distal ring occurs predominantly in the 1OH C-5 and C-8 positions.<sup>32,33</sup> Consequently, it was found that 1OH derivatives with electron-withdrawing substituents at C-5 and C-8 positions enhance their excited-state acidity.<sup>26,28</sup> It was however found that also the 2OH derivatives 5CN2OH and 8CN2OH have a much lower  $pK_a^*$  than 6- or 7-cyano-2-naphthols, 5CN2OH being the strongest photoacid (in water  $pK_a^* \approx -1.2$  as evaluated from Förster cycle and  $\approx -0.3$  from kinetic measurements).<sup>26,28</sup> It is interesting to note that, despite a great decrease of  $pK_a^*$  as compared to 2OH ( $\Delta pK_a^* \approx -3.0$ ), the ground-state  $pK_a$  (8.75, ref 26a) shows a more limited variation with substitution ( $\Delta pK_a \approx -0.7$ ), in accord with the ground-state charge distribution in naphthols as described above.

Protolytic photodissociation of 5CN2OH in pure methanol and water and in an array of neat organic solvents was studied by us extensively.<sup>28,29,34-36</sup> Thus this compound, like other cyanonaphthols,<sup>18,27</sup> seems to be a unique molecule for investigating protolytic dissociation over the full range of methanol/water composition. Pines et al. investigated the protolytic photodissociation of 5-cyano-1-naphthol (5CN1OH) in a wide range of methanol/water mixtures.<sup>18</sup> However, because of the poor signal-to-noise ratio due to very low  $R^*OH$  and  $R^*O^-$

fluorescence quantum yields, the kinetic curves were fitted using a biexponential function instead of the established diffusion approach.<sup>21,34,37</sup> Consequently, only the overall dissociation rate constant was determined, so the detailed mechanism of reversible geminate protolytic photodissociation of "super" photoacids in water/methanol mixtures remains unexplored.

The theory of geminate diffusion-influenced reactions has been successfully applied to the description of PTTS from 5CN2OH to pure water and methanol, as well as to other neat solvents.<sup>29,34,36</sup> However, the rates of dissociation and quenching by geminate protons in neat methanol were too slow to allow one to observe the full power-law asymptotic behavior predicted for  $R^*OH$  and  $R^*O^-$  (see Theory section).<sup>34,35</sup> On the other hand, in pure water the dissociation is extremely fast and the quenching effect is strong but, due to aggregation caused by low solubility, the long-time behavior is masked by the slowly decaying fluorescence of the aggregates. We have initiated this research with the hope that water/methanol mixtures will provide a reasonable compromise between the conflicting demands of solubility and reactivity. We hope to elucidate the PTTS mechanism in the methanol-rich region, where the properties of single water molecules may play a crucial role, and in the water-rich region where properties of the whole water network can be essential. Our work is also the first attempt to check whether proton photodissociation of hydroxyaromatic compounds in the whole range of methanol/water mixtures can be described by the Debye-Smoluchowski equation with the back-reaction boundary condition.<sup>21,34-36</sup> This mechanistic investigation is assisted by a measurement of H/D isotope effects on the kinetics of PTTS in MeOD/D<sub>2</sub>O mixtures.

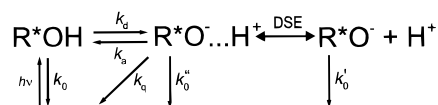
## II. Experimental Section

Experimental details were already described thoroughly in part 1 of this series.<sup>29</sup> Briefly, steady-state fluorescence spectra of nondeoxygenated 5CN2OH solutions were recorded on a SLM-AMINCO-Bowman 2 luminescence spectrometer. Fluorescence quantum yields were determined using dilute solutions of anthracene in aerated ethanol as a standard reference in a manner described in part 1.<sup>29</sup> Transient fluorescence was detected using time-correlated single-photon counting as described earlier.<sup>28,29</sup> A synchronized, cavity dumped picosecond Rhodamine 6G dye laser, driven by a Nd:YAG laser, was used as a source of excitation. The time-resolved signals from  $R^*OH$  and  $R^*O^-$  were detected at 370 and 570 nm, correspondingly. The time resolution varied from 4.88 to 97.7 ps/channel while the instrument response function (IRF) at the short time scales had a full-width at half-maximum of about 40 ps. 5CN2OH and other cyanonaphthols were synthesized and purified as described elsewhere.<sup>26</sup> The methanol solvent was BDH HPLC grade with <0.05% water. Deionized water (resistivity > 10 MΩ/cm) was used. D<sub>2</sub>O, 99.8% isotopically pure, and MeOD, 99.5% isotopically pure, were purchased from Aldrich. Solvents did not contain fluorescent impurities and were used without further purification. Methanol/water mixtures were prepared by the volumetric method. All experiments were performed at room temperature (ca. 22 °C).

## III. Theory

Our approach considers the proton-transfer process as a transient, nonequilibrium dissociation reaction of an excited-state molecule, using a two-step reaction model (Scheme 1).<sup>21,35,38</sup> Excitation of a solution at pH values lower than the ground-state  $pK_a$  of naphthol prepares, within a few hundred femtoseconds, a vibrationally relaxed, electronically excited

## SCHEME 1



ROH molecule (denoted by  $\text{R}^*\text{OH}$ ). Proton dissociation, with an intrinsic rate constant  $k_d$ , leads to formation of the contact ion pair (CIP)  $\text{R}^*\text{O}^-\cdots\text{H}^+$ , whereas adiabatic recombination with rate constant  $k_a$  may re-form the excited acid. In general, back protonation may proceed also by a nonadiabatic pathway, involving proton quenching with a rate constant  $k_q$ . Separation of a CIP from the contact radius,  $a$ , to infinity is described by the transient numerical solution of the Debye–Smoluchowski equation (DSE). Additionally, one should consider the fluorescence lifetimes of all excited species,  $1/k_0 = \tau_0$  for the acid,  $1/k_0' = \tau_0'$  for the base and  $1/k_0'' = \tau_0''$  for the CIP. Usually,  $k_0''$  is much slower than all chemical and diffusion processes and can be ignored.

Let us denote by  $p(^*,t|*)$  the probability of finding the initially bound pair at time  $t$  after excitation in its bound excited-state ( $\text{R}^*\text{OH}$ ), whereas  $p(r,t|*)$  denotes the probability density for the unbound excited pair to have a separation  $r \geq a$ . According to Scheme 1, the spherically symmetric DSE can be written as

$$\frac{\partial}{\partial t} p(r,t|*) = r^{-2} \frac{\partial}{\partial r} D r^2 e^{-V(r)} \frac{\partial}{\partial r} e^{V(r)} p(r,t|*) - [W_a(r) + W_q(r) + k_0'] p(r,t|*) + W_d(r) p(^*,t|*) \quad (2)$$

which is coupled to a kinetic equation for the bound state:

$$\frac{\partial}{\partial t} p(^*,t|*) = 4\pi \int W_a(r) p(r,t|*) r^2 dr - (k_d + k_0) p(^*,t|*) \quad (3)$$

$D = D_{\text{H}^+} + D_{\text{R}^*\text{O}^-}$  is the mutual diffusion coefficient of the proton and its conjugate base. The Coulomb attraction potential is  $V(r) = -R_D/r$ , where the Debye radius,  $R_D$ , at the temperature  $T$  is given by

$$R_D \equiv |z_1 z_2| e^2 / (k_B T \epsilon) \quad (4)$$

$z_1$  and  $z_2$  are the charges of the proton and the base and  $\epsilon$  is the static dielectric constant. “Sink terms” for association,  $W_a(r)$ , dissociation,  $W_d(r)$ , and geminate quenching,  $W_q(r)$ , refer to contact reactivity:

$$W_d(r) = \frac{k_d \delta(r-a)}{4\pi a^2}, \quad W_a(r) = \frac{k_a \delta(r-a)}{4\pi a^2}, \quad W_q(r) = \frac{k_q \delta(r-a)}{4\pi a^2} \quad (5)$$

Unlike electron-transfer reactions, there is no evidence for distance-dependent reactivity in PTTS. The time dependence of the survival probability of the excited anion is subsequently given by

$$S(t|*) = 4\pi \int_a^\infty p(r,t|*) r^2 dr \quad (6)$$

It was shown that geminate recombination leads to nonexponential decay of the  $\text{R}^*\text{OH}$  signal, whose asymptotic behavior is a power law, namely<sup>21,34,35</sup>

$$p(^*,t|*) \exp(k_0' t) \sim \frac{k_a \exp(R_D/a) Z^2}{k_d (4\pi D t)^{3/2}} \quad (7)$$

Recently we have demonstrated<sup>34,35</sup> that proton quenching and nonequal lifetimes of  $\text{R}^*\text{OH}$  and  $\text{R}^*\text{O}^-$  ( $k_0 \neq k_0'$ ) lead to a  $t^{-1/2}$  asymptotic decay of the  $\text{R}^*\text{O}^-$  signal

$$S(t|*) \exp(k_0' t) - Z \sim \frac{[(k_a + k_q)(k_0 - k_0') + k_q k_d] \exp(R_D/a) Z^2}{k_d (4\pi D) \sqrt{\pi D t}} \quad (8)$$

The ultimate escape probability  $Z$  is given by the formula<sup>34,35</sup>

$$Z = \frac{k_{\text{off}} k_{-D}}{(k_{\text{off}} + k_0 - k_0') k_{-D} + k_q k_{\text{off}}} \quad (9)$$

where the diffusional and overall separation rate coefficients are defined by

$$k_{-D} = \frac{4\pi D R_D}{\exp(R_D/a) - 1}, \quad k_{\text{off}} = \frac{k_d k_{-D}}{k_a + k_{-D} + k_q} \quad (10)$$

The excited-state  $\text{pK}_a^*$  can be calculated from the rate parameters according to

$$\text{pK}_a^* = -\log \frac{10^{27} k_d \exp(-R_D/a)}{k_a N_A} \quad (11)$$

The scaling factor  $10^{27}/N_A$  converts  $\text{\AA}^3/\text{ns}$  units into  $\text{mol (L s)}^{-1}$ .

In the present work we provide experimental evidence for the unusual nonexponential kinetics of 5CN2OH following its protolytic photodissociation in agreement with eqs 7 and 8. Specifically, we show the following:

(a) Both the acid and the base decay with the lifetime of the anion,  $\tau_0' \equiv 1/k_0'$ .

(b) The acid signal decays with the  $t^{-3/2}$  asymptotic law.

(c) Due to protolytic quenching, the anion signal,  $S(t|*) \exp(k_0' t)$ , goes through a maximum and approaches  $Z$  from above with a  $t^{-1/2}$  asymptotic law.

#### IV. Fitting Procedures

Experimental data were fitted to the numerical solution of the time-dependent DSE, eqs 2 and 3, using a Windows application for solving the spherically symmetric diffusion problem (SSDP version 2.55).<sup>37</sup> Details of the fitting procedure were described comprehensively in part 1,<sup>29</sup> so here we discuss briefly only those technical aspects which are specific to methanol/water mixtures. As in the previous work,<sup>29</sup> we have used only three adjustable kinetic parameters,  $k_d$ ,  $k_a$ , and  $k_q$ , to analyze the fluorescence decay curves of *both* acid and anion. The  $\text{R}^*\text{O}^-$  lifetimes found at long times at neutral pH and from a single-exponential decay fit of  $\text{R}^*\text{O}^-$  directly excited in basic solutions were identical. Other parameters were estimated from literature data as follows.

##### A. Parameter Determination. 1. The Interaction Potential.

For 5CN2OH at room temperature the Debye radius is  $R_D \equiv 566/\epsilon \text{ \AA}$ , according to eq 4. Figure 1 shows literature values for the static dielectric constant,  $\epsilon$ , of methanol/water mixtures.<sup>39–42</sup> We have found that these data (except ref 41) can be satisfactorily fitted by the polynomial ( $r = 0.997$ )

$$\epsilon(x) = 32.91 + 0.208x + 0.00246x^2 \quad (12)$$

where  $x$  is the molar fraction of water in methanol/water mixtures (Figure 1). Below, we use this formula to calculate the values of  $R_D$  in the methanol/water mixtures investigated.



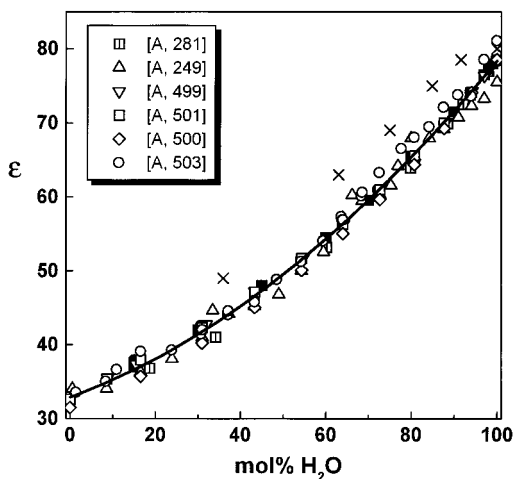


**Figure 1.** Dielectric constant of methanol/water mixtures. Closed circles, ref 39; closed squares, ref 40; crosses, ref 41. Open symbols, data from book of Akhador<sup>42</sup> [A, *n*] with *n* corresponding to reference numbers from this book. Solid line is the best polynomial fit, eq 12. See text for details.

The dielectric constants for CD<sub>3</sub>OD and D<sub>2</sub>O, are identical, within the error bars, to those of CH<sub>3</sub>OH and H<sub>2</sub>O.<sup>43</sup> Hence, we have used eq 12 also for deuterated methanol/water mixtures.

**2. The Diffusion Coefficients.** The mutual diffusion coefficient *D* is a sum of the proton (*D*<sub>H<sup>+</sup></sub>) and the naphtholate (*D*<sub>R<sup>•</sup>O<sup>-</sup></sub>) diffusion coefficients. The proton diffusion coefficient is estimated using the Nernst equation<sup>44</sup>

$$D_{H^+} = RT\lambda^0/F^2 \quad (13)$$

where  $\lambda^0$  is the limiting proton mobility and *F* is Faraday's constant. For  $\lambda^0$  in units of Ω<sup>-1</sup> cm<sup>2</sup> equiv<sup>-1</sup>

$$D_{H^+} = 2.66 \times 10^{-7} \lambda^0 \text{ (cm}^2/\text{s)} \quad (14)$$

at 25 °C. The limiting proton mobility was estimated from electrochemical data on equivalent conductivity of hydrochloric acid and transference number of protons in methanol/water mixtures.<sup>45</sup> The naphtholate diffusion coefficient (*D*<sub>R<sup>•</sup>O<sup>-</sup></sub>, 1.13 × 10<sup>-5</sup> cm<sup>2</sup>/s) used by Weller<sup>46</sup> and others<sup>47</sup> seems too large for the conjugated base of 5CN2OH. Diffusion coefficients of aromatic compounds in aqueous solutions (*D*<sub>R<sup>•</sup>O<sup>-</sup>,H<sub>2</sub>O</sub>) usually do not exceed 0.95 × 10<sup>-5</sup> cm<sup>2</sup>/s.<sup>48</sup> In our work we use the value of 0.75 × 10<sup>-5</sup> cm<sup>2</sup>/s for the diffusion coefficient of the 5CN2OH anion in water, as evaluated from experimental data of various substituted naphthalenes.<sup>49</sup> Values of diffusion coefficients in methanol/water mixtures (*D*<sub>R<sup>•</sup>O<sup>-</sup></sub>) were assumed to be directly proportional to the viscosity ratio of water and the mixture<sup>50</sup> ( $\eta_{H_2O}/\eta$ ):

$$D_{R^{\bullet}O^-} = D_{R^{\bullet}O^-,H_2O} \eta_{H_2O}/\eta \quad (15)$$

The dependence of the diffusion coefficients on mixture compositions is shown in Figure 2.

To determine the values of *D* in MeOD/D<sub>2</sub>O mixtures, we consider the possible influence of deuteration on both *D*<sub>H<sup>+</sup></sub> and *D*<sub>R<sup>•</sup>O<sup>-</sup></sub>. In water the isotopic mobility ratio is  $\lambda_{H^+}/\lambda_{D^+} = \sqrt{2}$ .<sup>43</sup> As this ratio in methanol is unknown, we have assumed that  $D_{H^+}/D_{D^+} = \sqrt{2}$  at all water concentrations. The diffusion coefficient of R<sup>•</sup>O<sup>-</sup> was estimated using the known values of  $\eta_{D_2O}/\eta_{H_2O}$  (1.2, ref 43) and  $\eta_{MeOD}/\eta_{MeOH}$  (1.1, estimated from average solvation times of the MeOD dipole in ref 51).

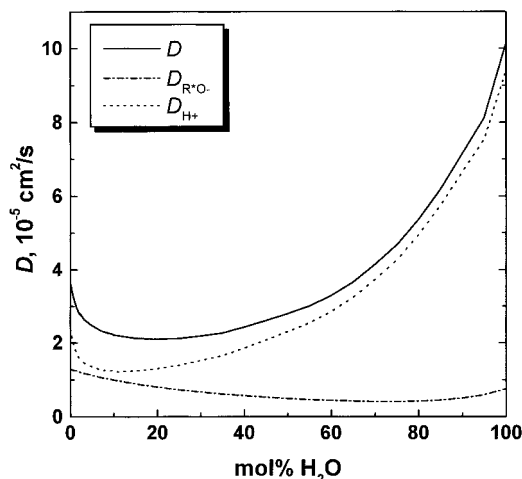


**Figure 2.** Diffusion coefficients of the proton, naphtholate anion, and their sum in methanol/water mixtures.

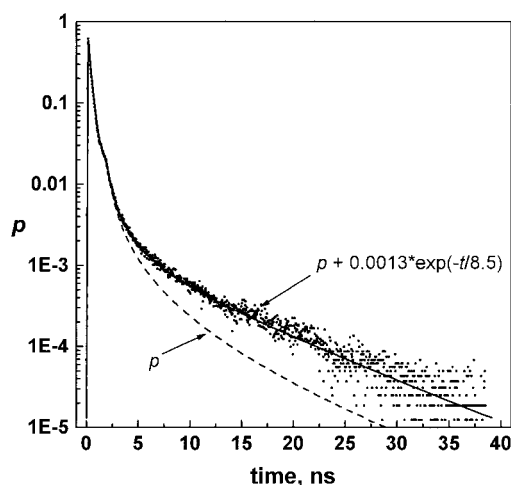


**Figure 3.** Time-resolved kinetics of 5CN2OH in 25.3 mol % aqueous methanol. Experimental R<sup>•</sup>OH signal (points, normalized to the theoretical amplitudes) are compared with the numerical solution of the DSE (lines) after convolution with the IRF. The solid line takes into account a small fraction of impurity (see text for details).

**B. Data Correction for Band Overlap, Background, and Impurities.** As mentioned in our previous publications,<sup>28,29</sup> at high water contents R<sup>•</sup>OH fluorescence exhibits a long-lived component not related to protolytic photodissociation. Its contribution increases with increasing water content from 0.03% at 3 mol % water up to 0.3% at 90 mol % water and even higher in pure water. Since the lifetime of this component (8 ± 1 ns) is shorter than that of R<sup>•</sup>O<sup>-</sup>, it cannot be attributed to the appearance of the R<sup>•</sup>O<sup>-</sup> signal at 375 ± 5 nm. This long-lived component does not influence the initial fast decay of R<sup>•</sup>OH which is governed mainly by *k*<sub>d</sub> and *k*<sub>a</sub>. Figure 3 demonstrates the subtraction of this component from the decay curves of R<sup>•</sup>OH in 25.3 mol % aqueous methanol solution. As in our previous study<sup>28,29</sup> we attribute this component to (a) oligomers of 5CN2OH whose solubility decreases significantly from methanol to water, (b) impurities which do not undergo PTTS, for example, the precursor in the multistep synthesis of 5CN2OH, namely 5-cyano-2-methoxynaphthalene,<sup>26</sup> or (c) slight decomposition of the original compound.

## V. Results and Discussion

**A. Steady-State Spectra.** Emission spectra of monocyano derivatives of 2-naphthol in methanol are presented in Figure

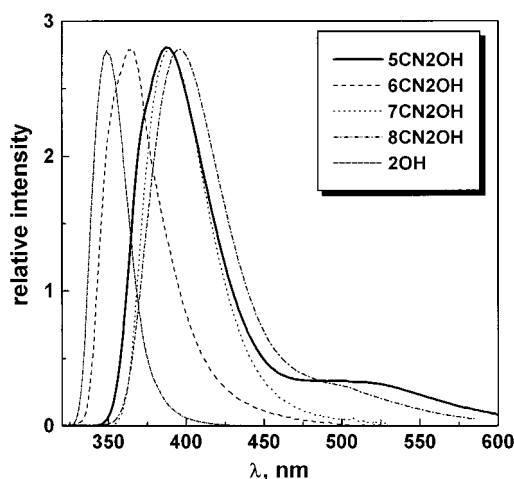


**Figure 4.** Fluorescence spectra of cyanoderivatives of 2-naphthol in methanol. Spectrum of 2-naphthol (most blue-shifted) is given for comparison.

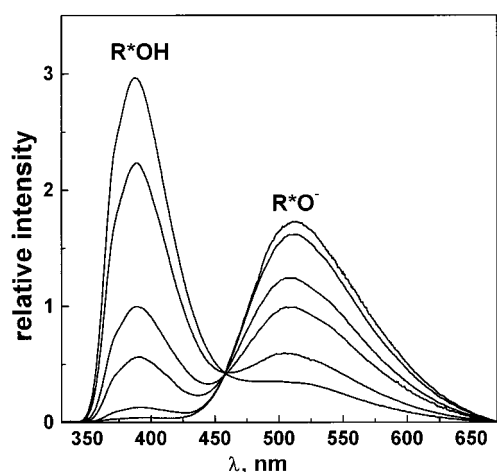


**Figure 5.** Fluorescence spectra of 5CN2OH in methanol/water mixtures. Water content (for R\*OH band, from top to bottom) is 0, 1.78, 6.75, 11.2, 25.3, and 47.5 mol %.

4. The appearance of the low energy ( $R^*O^-$ ) emission band at 500 nm for 5CN2OH and 8CN2OH indicates an efficient PTTS process. The largest ratio of the  $R^*O^-$ -to- $R^*OH$  intensities for 5CN2OH reflects the highest reactivity of this compound among this family of cyanonaphthols. This reactivity order is corroborated time-resolved data.<sup>28</sup> With the exception of 8CN2OH, it appears that the photoacidity correlates with the red-shift of the  $R^*OH$  band. A possible explanation for this exception could be a solvent-bridged intramolecular hydrogen bond between hydroxylic and cyano groups, whose cleavage is a prerequisite for PTTS in 8CN2OH. A similar bridge was proposed for other bifunctional compounds, such as 7-azaindole<sup>52</sup> and 7-hydroxyquinoline.<sup>53</sup>

The emission spectra of 5CN2OH in methanol–water mixtures of several concentrations are shown in Figure 5. All spectra were normalized to equal absorbance at the excitation wavelength, 304 nm. Hence the isoemissive point observed in the methanol-rich region is a real effect. With the increase of water content in the mixtures, we observe a substantial decrease of the fluorescence intensity of the nondissociated form of naphthol at 390 nm and a concomitant increase of naphtholate intensity at 510 nm. This well-known effect in hydroxyaromatic compounds<sup>2–18</sup> is attributed to the increase of the protolytic photodissociation rate with increasing water concentration. Only a very small bathochromic shift was observed for both  $RO^*H$

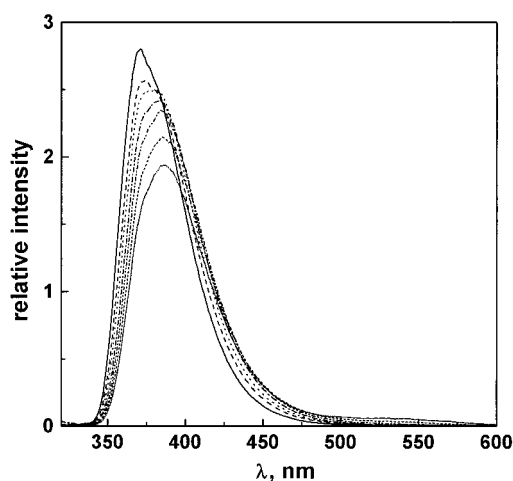


**Figure 6.** Fluorescence spectra of 5CN2OH in acetonitrile/water mixtures. Water content (top to bottom) is 0, 1.2, 2.3, 3.9, 5.5, 7.1, and 8.5 mol %. A weak  $R^*O^-$  signal appears in the last spectrum.

and  $R^*O^-$  bands as the water concentration increased.<sup>29,54</sup> Therefore, there is no spectral evidence for preferential solvation of 5CN2OH in methanol/water solutions.

Note, however, that changing the organic cosolvent can lead to a sizable preferential solvation as evidenced in the spectral shift. Upon addition of *small* amounts of water (up to ca. 5 mol %) to acetonitrile solutions of 5CN2OH, a pronounced bathochromic shift (without the appearance of  $R^*O^-$  fluorescence) is observed in the fluorescence spectra (Figure 6). This indicates preferential solvation of cyanonaphthol by water molecules through hydrogen-bonding and dipole–solvent interactions. Despite the small intensity decrease (Figure 6), no change in fluorescence quantum yield and lifetime of  $R^*OH$  is observed (data not presented). It is interesting to note that the fluorescence of  $R^*O^-$  was only observed above a certain minimal water concentration (8.5 mol %), when the wavelength of  $R^*OH$  emission maximum approaches its value in neat alcohols (386 nm).<sup>29</sup> With the additional increase of water concentration above 10 mol % no further change in the position of the  $R^*OH$  emission maximum was observed.

**B. Time-Resolved Fluorescence.** Figure 7 shows time-resolved fluorescence of 5CN2OH in methanol/water compositions corresponding to the steady-state spectra shown in Figure 5. The decaying curves correspond to the  $R^*OH$  signal [ $I(t) = p(t^*),$  eq 2], whereas the rising curves are the  $R^*O^-$  signal [ $I(t) = S(t^*),$  eq 6]. The data (dots) are processed as described in part 1<sup>29</sup> and in section IV.B and multiplied by  $\exp(t/\tau_0')$ . The theoretical curves (lines) represent the numerical solution of eqs 2 and 3 with appropriate parameters collected in Table 1. Only the three rate coefficients,  $k_d$ ,  $k_a$ , and  $k_q$ , were used as adjustable parameters. Analogous data in MeOD/ $D_2O$  solutions are given in Table 2. The experimental data were convoluted with IRF and normalized to the absolute intensities of the theoretical signal.

At low water concentrations the effective anion signal rises and approaches the ultimate escape probability  $Z$  of eq 9 (dash–dotted lines). With the increase of water content,  $S(t^*) \exp(t/\tau_0')$  reaches a peak and then approaches  $Z$  from above. This effect, attributed to contact quenching by the geminate proton, was previously observed for 1-naphthol.<sup>55</sup> However, due to the absence of appropriate theory,<sup>35</sup> the data has not been analyzed asymptotically using eqs 7 and 8.

The diffusive mechanism underlying the PTTS process is expected to result in the asymptotic power laws for  $R^*OH$  and

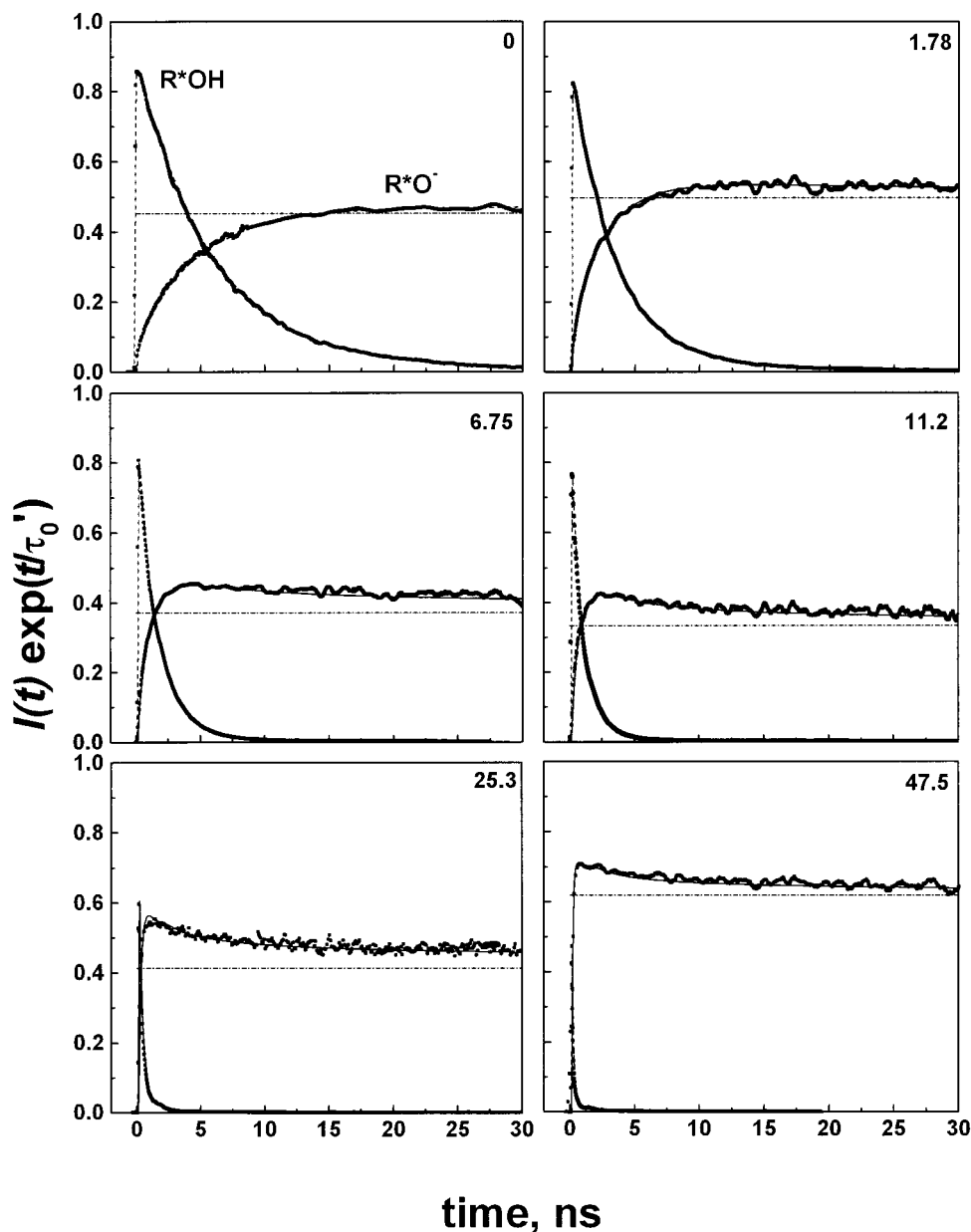


**Figure 7.** Time-resolved kinetics of 5CN2OH in methanol/water mixtures of the same concentrations as in Figure 5. Experimental fluorescence data for both acid and anion (points, normalized to the theoretical amplitudes) are compared with the numerical solution of the DSE (dashed lines,  $R^*OH$ ; full lines,  $R^*O^-$ ), using the parameters of Table 1, and after convolution with the IRF. All lines are corrected for the lifetime of the anion. The dash-dotted lines are the ultimate dissociation probabilities,  $Z$ , from eq 9.

$R^*O^-$  signals as depicted in eqs 7 and 8, respectively. To demonstrate this, we replot one pair of  $[R^*OH] \exp(t/\tau_0')$  and  $[R^*O^-] \exp(t/\tau_0') - Z$  curves on a log-log scale in Figure 8. Both experiment (points) and theory (full lines) approach the power-law limits predicted by eqs 7 and 8 (dash-dot lines) during the excited-state lifetimes of acid and base: The acid decays as  $t^{-3/2}$  whereas the base decays with the  $t^{-1/2}$  law. Similar power-law asymptotics were observed for other solvent compositions. Figure 9 demonstrates this for the  $R^*OH$  time-resolved data. It is obvious that after correction for the base fluorescence lifetime,  $\tau_0'$ , all data follow the ubiquitous  $t^{-3/2}$  asymptotic law (dash-dotted lines).

In the water-rich region, starting from ca. 50 mol %  $H_2O$ , the accuracy of the determination of the PTTS rate constant decreases. The dissociation rate increases and approaches the time resolution of our single-photon counting system (see Experimental Section). 5CN2OH aggregation and impurities (Figure 3) mask the effect of geminate recombination and,

therefore, hinder the accurate determination of  $k_a$  and  $k_q$ . Although the  $R^*O^-$  signal can be easily detected in this solvent region, the  $t^{-1/2}$  nonexponential decay is hardly seen because the quenching reaction now occurs within the IRF. Thus time-resolution limits the accuracy of our measurements in the water-rich region.

**C. Free-Energy Relationship.** The dissociation rate coefficient,  $k_a$ , depends nonlinearly on the mole fraction of water (Figure 10), showing strong variation in the methanol-rich region and changing very little in the 0–60% MeOH region. A similar effect was observed for 5CN1OH.<sup>18</sup> It was explained by (a) preferential solvation of the hydroxyl moiety by water and (b) gradual change in the solvation energy of the CIP.

We have analyzed the dependence of the dissociation rate constant on the free energy of the reaction. In contrast to the  $k_a$ –MeOH% relation, the Brønsted-type dependence in the log  $k_a$ – $pK_a^*$  coordinates shows only a slight deviation from a slope of  $-1$  in water-rich solutions (Figure 11). Several workers<sup>1d,17,56</sup>

**TABLE 1: Parameters Used in Fitting the Time-Resolved Fluorescence Decay of 5CN2OH to Eqs 2 and 3 and Calculated  $pK_a^*$  Values in MeOH/H<sub>2</sub>O Mixtures<sup>a</sup>**

mol % H <sub>2</sub> O	vol % H <sub>2</sub> O	$k_d$ , 1/ns	$k_a/4\pi a^2$ , Å/ns	$k_q/4\pi a^2$ , Å/ns	$\tau_0'$ , ns	$D$ , 10 <sup>-5</sup> cm <sup>2</sup> /s	$R_D$ , Å	$pK_a^*$
0	0	0.22	16.0	2.3	10.15	3.66	17.20	2.58
0.90	0.40	0.42	15.3	3	10.1	3.15	17.10	2.27
1.78	0.79	0.55	15.3	4	10.2	2.86	17.00	2.15
2.64	1.19	0.63	14.7	6.8	10.7	2.74	16.91	2.06
3.49	1.57	0.75	14.9	8	10.7	2.61	16.81	1.98
4.33	1.96	0.91	15.6	9	10.7	2.54	16.72	1.91
5.15	2.34	1.05	15.4	9.2	10.7	2.47	16.63	1.84
6.75	3.10	1.21	15.0	9.3	10.9	2.36	16.44	1.75
8.29	3.85	1.47	15.5	9.7	11	2.29	16.26	1.67
9.05	4.21	1.61	15.6	10.5	11	2.27	16.17	1.62
9.79	4.58	1.79	13.5	10.5	11.2	2.24	16.09	1.51
10.5	4.94	1.95	15.0	11	11.2	2.21	16.00	1.51
11.2	5.30	2.0	15.0	11	11.2	2.20	15.91	1.49
11.9	5.66	2.2	14.3	12	11.2	2.19	15.84	1.42
14.5	6.98	3.0	15.7	12	11.7	2.14	15.53	1.30
25.3	13.1	6.3	17	12	12.9	2.12	14.23	0.91
33.7	18.4	9.9	19	13	13.9	2.25	13.25	0.69
40.4	23.1	13.5	20	12	14.3	2.47	12.49	0.52
47.5	28.6	15.4	21	11	14.3	2.7	11.71	0.42
60.1	40	18.5	22	13	14.5	3.3	10.42	0.26
69.3	50	21	23	13	13.2	4.07	9.57	0.15
87.1	75	28	26	12	9.4	6.6	8.13	-0.03
95.3	90	33	28	12	7.4	8.25	7.54	-0.12
98.3	96.2	45	26	11	7.25	11	7.28	-0.30

<sup>a</sup> At all concentrations we have taken  $a = 5.5$  Å and  $\tau_0 = 5.7$  ns. Due to our finite time resolution, experimental errors are considerably larger in the water-rich region.

**TABLE 2: Parameters Used in Fitting the Time-Resolved Fluorescence Decay of 5CN2OH to Eqs 2 and 3 and Calculated  $pK_a^*$  Values in MeOD/D<sub>2</sub>O Mixtures<sup>a</sup>**

mol % D <sub>2</sub> O	$k_d$ , 1/ns	$k_a/4\pi a^2$ , Å/ns	$k_q/4\pi a^2$ , Å/ns	$\tau_0$ , ns	$\tau_0'$ , ns	$D$ , 10 <sup>-5</sup> cm <sup>2</sup> /s	$R_D$ , Å	$pK_a^*$
0	0.097	11.2	0.7	6.2	11.6	2.75	17.2	2.78
2.19	0.18	11.4	2	5.8	12	2.13	16.96	2.50
4.81	0.38	11.7	3.5	5.8	12.6	1.91	16.66	2.16
7.76	0.61	11.8	6	6	13.4	1.76	16.38	1.94
12.3	1.01	12	7.7	5.8	14.4	1.65	15.71	1.67
17.4	1.7	12.4	7.5	5.7	15.6	1.6	15.18	1.42
24.4	2.85	12.6	8	5.7	17.1	1.59	14.34	1.14
32.9	3.8	12.8	9	5.7	18.9	1.66	13.34	0.94
41.2	5.0	12.8	9	5.7	19.7	1.81	12.4	0.75
49.5	6.3	13	9	5.7	21.5	2.02	11.5	0.58
59.6	7.8	13.1	9	5.7	21.9	2.36	10.47	0.41
62.9	8.8	13	8	5.7	22	2.53	10.16	0.33
69.2	9.3	13.3	8	5.7	22	2.93	9.57	0.27
73.7	10.5	13.3	8	5.7	22	3.25	9.19	0.19
77.1	12.4	13.4	8	5.7	21.3	3.56	8.91	0.10
84.0	14.6	13.5	8	5.7	19.7	4.31	8.36	-0.015
90.5	17.5	16	8	5.7	17.7	5.2	7.87	-0.06
95.3	19	16	8	5.7	16.5	5.8	7.53	-0.12
97.8	21	17	8	5.7	15.5	6.7	7.36	-0.15

<sup>a</sup> At all concentrations we have taken  $a = 5.5$  Å. Due to our finite time resolution, experimental errors are considerably larger in the water-rich region.

have correlated  $k_d$  for various photoacids with their  $pK_a^*$ , using a procedure suggested by Marcus<sup>57</sup> and Agmon and Levine.<sup>58</sup> The basic assumption in this approach is that within a family of similar reactions the free-energy barrier varies smoothly with the total free-energy change of the reaction. In our case we have

$$\Delta G = -RT \ln K_a^* \quad (16)$$

for the total free-energy change, where  $K_a^*$  is given by eq 11.

The measured dissociation constants are assumed to obey an Arrhenius relation:

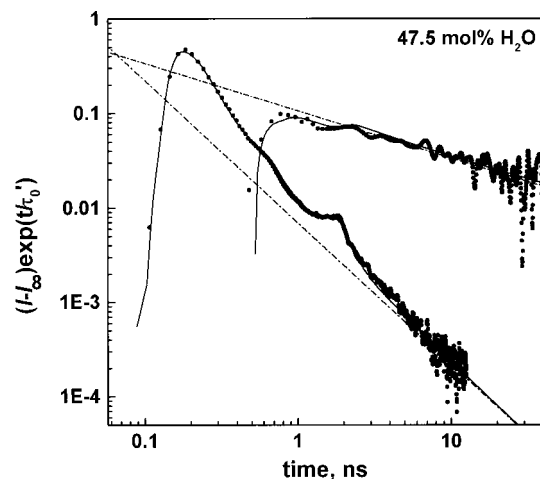


**Figure 8.** Data for 47.5 mol % H<sub>2</sub>O from Figure 7 portrayed on a log–log scale. Dash–dotted lines are asymptotic behaviors from eqs 7 and 8. Full line is the numerical solution of eqs 2 and 3, convoluted with the IRF. The wiggle near 1.5 ns is due to a parasitic excitation afterpulse.

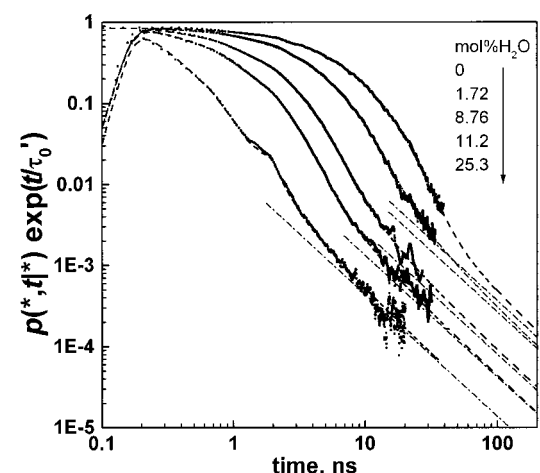


**Figure 9.** Time-resolved kinetics of 5CN2OH R\*OH band in methanol/water mixtures of the same composition as in Figure 5 are displayed on a log–log scale.

$$k_d = k_d^\circ \exp\left[-\frac{G_a}{RT}\right] \quad (17)$$

where the free-energy barrier for reaction,  $G_a$ , depends on  $\Delta G$  and on some intrinsic barrier  $G_a^\circ$ , defined as  $G_a$  for a symmetric ( $\Delta G = 0$ ) reaction in the series<sup>58</sup>

$$G_a = \Delta G - G_a^\circ \ln(n^\#)/\ln(2) \quad (18)$$

Here  $n^\#$  is the location of the reaction barrier along the proton coordinate:  $n^\# = 0$  (reactant like) for the endothermic limit and  $n^\# = 1$  (product like) for the exothermic one. It is given by

$$n^\# = \left[1 + \exp\left(\frac{-\Delta G \ln(2)}{G_a^\circ}\right)\right]^{-1} \quad (19)$$

The use of structure–reactivity correlations for different aromatic photoacids is summarized by Arnaut and Formosinho,<sup>1d</sup> who find  $G_a^\circ = 1.9$  kcal/mol. Pines et al.<sup>56</sup> found  $k_d^\circ = 2 \times 10^{11}$  s<sup>-1</sup> and  $G_a^\circ = 2.5$  kcal/mol, whereas for a single compound, 5CN1OH, in various methanol/water mixtures, the values of  $k_d^\circ = 2.5 \times 10^{11}$  s<sup>-1</sup> and  $G_a^\circ = 1.6$  kcal/mol were obtained.<sup>18</sup> This places the activationless limit of proton transfer in water,



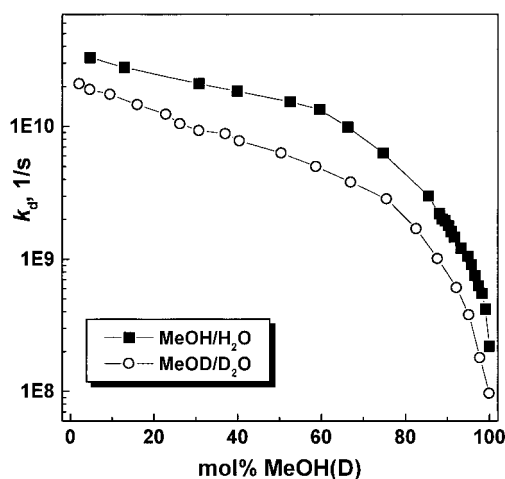


Figure 10. Dependence of dissociation rate constant on solvent composition.

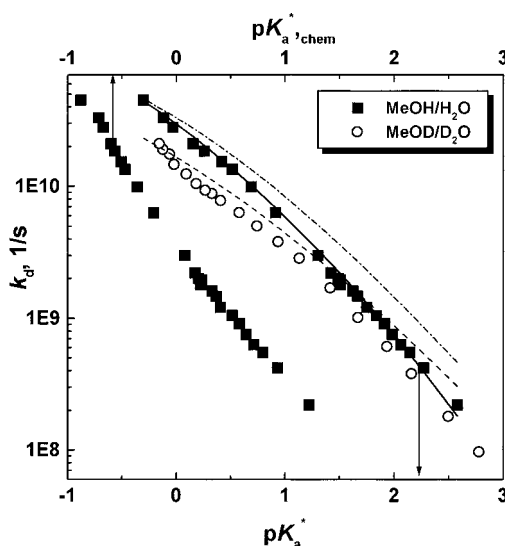


Figure 11. Brønsted-type dependence of  $\log k_d$  on the  $pK_a^*$ . Parameters of the free-energy correlations (lines) are given in the text. Upper X-axis refers to the "chemical"  $pK_a^*$ .

$1/k_d^\circ = 4$  ps, between the Debye relaxation time ( $\tau_D \approx 8$  ps for water at 25 °C) and the longitudinal relaxation time,  $\tau_L = (\epsilon_\infty/\epsilon_s)\tau_D \approx 0.5$  ps, where  $\epsilon_\infty$  and  $\epsilon_s$  are the dielectric constants of the solvent at "infinite" and zero frequencies, respectively.

We find that our data in MeOH/H<sub>2</sub>O mixtures (Figure 11) do not fit well using  $k_d^\circ = 2.5 \times 10^{11} \text{ s}^{-1}$  and either  $G_a^\circ = 1.7$  kcal/mol (dashed line) or  $G_a^\circ = 1.2$  kcal/mol (dash-dot line). The solid line in Figure 11 shows a fit to eqs 16–19 using a solvent-dependent preexponential factor,  $k_d^\circ = 3.37 \times 10^{11} - 2.35 \times 10^{10} pK_a^* \text{ s}^{-1}$ , and  $G_a^\circ = 1.4$  kcal/mol. Comparison of the two cyanonaphthols shows that the 5CN2OH data are still far from the "ultimate" dissociation limit,  $1/k_d^\circ \sim 3$  ps.

A related question concerns the value of the intrinsic barrier and whether it should equal the activation energy of proton mobility in water (2.5 kcal/mol).<sup>39,44</sup> Assuming water always to be the proton acceptor, the symmetric case,  $G_a = G_a^\circ$ , might correspond to  $\text{H}_3\text{O}^+ + \text{H}_2\text{O} \rightleftharpoons \text{H}_2\text{O} + \text{H}_3\text{O}^+$ . While the correlation with  $pK_a^*$  yields, as in the case of 5CN1OH in methanol/water mixtures,<sup>18</sup> a smaller  $G_a^\circ$  value than 2.5 kcal/mol, the need to introduce a  $pK_a^*$ -dependent  $k_d^\circ$  questions this approach: The small curvature in the structure–reactivity correlation could arise from a variation of the dielectric constant of the mixture.

To address this problem, it is perhaps preferable to eliminate first the electrostatic contribution (the Marcus "work terms") from the overall  $pK_a^*$  values according to

$$pK_{a,\text{chem}}^* = pK_a^* - R_D/2.303a = -\log(k_d/k_a) \quad (20)$$

Such an approach has enabled the comparison of sulfonated hydroxyaromatic compounds of different charge.<sup>17</sup> Plotting the dependence of 5CN2OH  $k_d$  vs  $pK_{a,\text{chem}}^*$  (Figure 11, upper X-axis) gives a slope of  $\sim 1$  for the whole data set, showing that indeed the nonlinearity of this dependence in the  $\log k_d$ – $pK_a^*$  coordinates is caused by electrostatic factors. PTTS for 5CN2OH is in the endothermic regime for all methanol/water concentrations, and thus the determination of the intrinsic barrier requires even stronger photoacids.

**D. Isotope Effects.** The isotope effect on the photodissociation rate of the "super" photoacids was investigated earlier in pure water and methanol<sup>27,28</sup> and their mixtures.<sup>18</sup> With decreasing  $pK_a^*$  (i.e., increasing water content), this reaction exhibits a transition from activation control to solvent control, manifested in a decrease of the isotope effect on  $k_d$ , from 2.6 to 1.6. 5CN2OH is less acidic than 5CN1OH and its protolytic photodissociation in water is far from the activationless limit (Figure 11). The isotope effect for  $k_d$  (Tables 1 and 2) is practically constant ( $2.2 \pm 0.2$ ) in the region 0–80 mol % MeOH. The error in its determination in the methanol-rich region is large because uncertainties in  $k_0$  lead to larger errors in the determination of  $k_d$  in MeOD/D<sub>2</sub>O solutions as compared with MeOH/H<sub>2</sub>O. Our data also confirm the finding of Huppert et al.<sup>28</sup> that the isotope effect is larger for  $k_d$  than for  $k_a$ . The isotope effect on  $k_a$  varies here between 1.3 and 1.7, roughly equal to the isotope effect for proton mobility (1.4).<sup>39,44</sup> These values suggest a small barrier for proton dissociation and no barrier for its recombination, in agreement with our observation from the structure–reactivity correlation that the reaction is in the endothermic regime.

**E. Nature of Proton Acceptor.** One of the most intriguing questions in protolytic photodissociation research is the nature of the primary proton acceptor. Analysis of time-resolved studies of the protolytic dissociation of various naphthols in mixed alcohol/water solutions shows a broad variation in the number of water molecules in the acceptor cluster. Robinson et al.<sup>5–7,14</sup> suggested that a water tetramer is an effective proton acceptor for both weak (2OH) and strong (1OH) photoexcited acids. Klein et al.<sup>11</sup> have found that the a water dimer is an effective proton acceptor for the dissociation of 4S1OH in alcohol–water mixtures. Agmon et al.<sup>9</sup> suggested that the proton is solvated in the water-rich region by a single water molecule, with either water or methanol in the  $\text{H}_3\text{O}^+$  solvation shell. It was proposed by Tolbert<sup>26b</sup> that the apparent size of the water cluster decreases with the increase of photoacid strength.

Use of super photoacids allows us to investigate the situation in the methanol-rich region. If we assume that PTTS to water and methanol can be considered as two parallel processes, then the nature of the proton-accepting water cluster can be determined by an analysis of the dissociation constant dependence on water concentration using

$$k_d = k_m + k_w[\text{H}_2\text{O}]^n \quad (21)$$

where  $k_m$  is the dissociation rate in pure methanol and  $k_w$  is its water-dependent component. The kinetic order parameter,  $n$ , can be roughly associated with the number of water molecules involved in the proton-transfer step. Note that near pure methanol (say, mol % water  $\leq 10\%$ ) the dielectric constant of



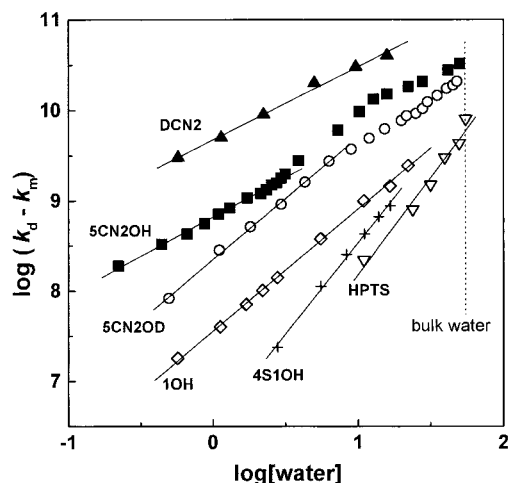


**Figure 12.** Dependence of proton photodissociation rate coefficient (in  $\text{s}^{-1}$ ) on molar water concentration in methanol/water mixtures for various naphthols according to eq 22. See Table 3.

**TABLE 3: Slopes of Dependences According to Eq 22 for Various Hydroxyaromatic Compounds in Methanol/Water Mixtures**

compound	$\text{p}K_{\text{a}}^*$ <sup>a</sup>	$k_{\text{w}}$ , 1/ns	$k_{\text{m}}$ , 1/ns	$n$	ref
DCN2	$\sim -4$	4.7	10	$0.81 \pm 0.03$	60
5CN2OH/H <sub>2</sub> O	-0.3	0.66	0.22	$0.87 \pm 0.02$	this work
5CN2OH/D <sub>2</sub> O	-0.15	0.22	0.097	$1.35 \pm 0.02$	this work
1OH	0.4	0.036	0	$1.35 \pm 0.02$	9
HPTS	1.3	0.0016	0	$2.00 \pm 0.13$	9
4S1OH	-0.1	0.0032	0	$2.02 \pm 0.04$	11a

<sup>a</sup> In water.

the solution hardly changes (Figure 1), so the electrostatic stabilization of the anion (which plays an important role in the water-rich region)<sup>9</sup> is not a dominant factor. We plot the photodissociation rate constant as a function of water concentration according to

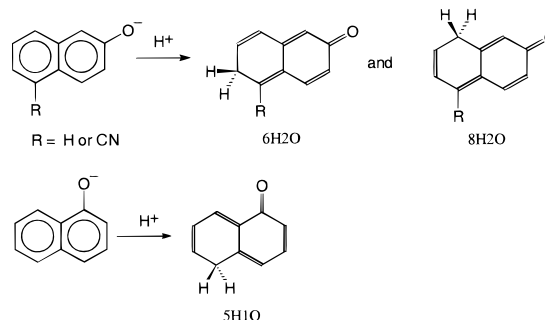
$$\log(k_{\text{d}} - k_{\text{m}}) = \log k_{\text{w}} + n \log [\text{H}_2\text{O}] \quad (22)$$

in Figure 12. The results of the linear fit are summarized in Table 3.

The data collected in Figure 12 and Table 3 provide a first clear demonstration for the decrease of  $n$  with increasing photoacidity. Therefore  $n$  cannot depict the water cluster size solvating the proton in bulk methanol/water, which should be independent of the photoacid. A more reasonable assumption is that  $n$  reflects the structure of the CIP.<sup>53</sup> It was suggested<sup>59</sup> that this transient complex, in water, involves a  $\text{H}_5\text{O}_2^+$  ion bridged to the anion by two water molecules. Assuming linear extrapolation of the lines in Figure 12, it appears, from Table 3, that the weaker photoacids strive to preserve the  $\text{H}_5\text{O}_2^+$  moiety in the CIP at high methanol contents. "Super" photoacids, in comparison, may tolerate a smaller number of water molecules in their CIP. The latter may approach the acid dissociation mechanism investigated by Ando and Hynes,<sup>61</sup> where  $\text{H}_3\text{O}^+$  is formed in the first and then the second solvation shell of the anion. Hence with increasing photoacidity the structure of the CIP undergoes a transition,<sup>26b</sup> from  $\text{H}_5\text{O}_2^+$  to  $\text{H}_3\text{O}^+$  in the second solvation shell of the  $\text{R}^*\text{O}^-$ .

**F. Proton-Induced Quenching.** In this study, a significant 5CN2OH fluorescence quenching by geminate protons at neutral pH has been found. This is evident from the appearance of the maximum in the  $\text{R}^*\text{O}^-$  fluorescence signal in Figure 7 (see subsection B).

## SCHEME 2



It is important to note that there are two alternative mechanisms of  $\text{R}^*\text{O}^-$  nonadiabatic protonation. One refers to the protonation of a carbon atom of the naphthalene ring,<sup>32,33</sup> while the other involves<sup>3,22a,62</sup> proton *recombination-induced deactivation* to the ground state. This radiationless process competing with proton transfer in a reactive hydrogen-bonded complex is caused by the appearance of new modes promoting an efficient internal conversion in the vicinity of the reaction's transition state. Kuz'min and co-workers suggested<sup>22a,62</sup> that the latter process can be especially effective in two cases: First is the presence of two close-lying excited states,  $^1\text{L}_{\text{b}}$  and  $^1\text{L}_{\text{a}}$  as in the case of 1-naphthol and 1-naphthylamine, and their possible inversion upon excitation.<sup>62a</sup> Second is the case of large differences between the ground- and excited-state  $\text{RO}^-$  dipole moments, as observed for 1-naphtholate in water.<sup>62c</sup> We do not have evidence of a dramatic increase of the 5CN2O<sup>-</sup> dipole moment upon excitation. In addition, the shape of the absorption and fluorescence spectra of 5CN2OH do not differ from that of 2-naphthol, suggesting a similar electronic structure, or, at least, nonmixing of  $^1\text{L}_{\text{b}}$  and  $^1\text{L}_{\text{a}}$  states. Therefore, as in 2OH, recombination-induced deactivation has a minor importance for nonadiabatic protonation of 5CN2OH.

It is interesting to compare the quenching processes in 5CN2OH and 2OH. No quenching by geminate protons was reported for the excited 2OH anion. We believe, however, that the relatively slow protolytic photodissociation of 2OH in water does not allow one to observe the nonadiabatic recombination in the time-resolved signal of either  $\text{R}^*\text{OH}$  and  $\text{R}^*\text{O}^-$ . Indeed, the efficiency of adiabatic protonation,  $\phi = k_{\text{a}}/(k_{\text{a}} + k_{\text{q}})$ , by homogeneous protons (0.73–0.8)<sup>63a,64</sup> in water is surprisingly close to the value obtained in the present work for 5CN2O<sup>-</sup> quenching by geminate protons (Table 1). Both values are much higher than for 1OH ( $\sim 0.3$ ).<sup>55,63b</sup> More efficient proton quenching in 1OH derivatives was explained by Webb et al.<sup>33</sup> on the basis of a MNDO calculation. They demonstrated that the excited state protonation of the naphthalene ring is exothermic for 5H1O formation and endothermic for 6H2O and 8H2O ( $\text{R} = \text{H}$ ) formation (Scheme 2). A detailed scheme of proton-induced fluorescence quenching of 2-naphthol derivatives shows that C-5 substitution does not influence directly the C-6 and C-8 positions, which are supposed to be the most probable sites for electrophilic attack on the distal ring (Scheme 2). The similarity of  $\phi$  for 2OH and 5CN2OH indeed suggests that their quenching mechanism is similar. Alternatively, Tolbert and Haubrich have proposed that protonation of the cyano group can be effective in the case of cyanonaphthols.<sup>26b</sup> However, Shizuka demonstrated<sup>32</sup> that the rate constants of proton quenching of 1- and 2-cyanonaphthalenes are 2 orders of magnitude smaller than those of hydroxy- and methoxynaphthalenes. Accordingly, the cyano group plays only a minor role in the quenching process.

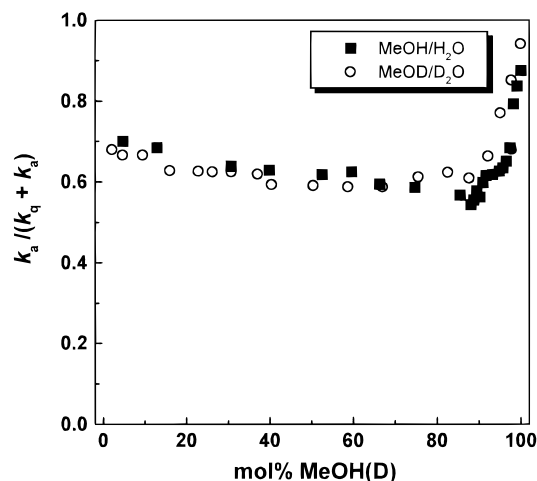


**Figure 13.** Efficiency of adiabatic vs diabatic protonation of  $R^*O^-$  in methanol/water mixtures.

We have found a unique dependence of  $\phi$  on water concentration in methanol/water mixtures. The efficiency of adiabatic protonation decreases sharply with the increase of water content from 0 up to 10 mol % and remains almost constant with further addition of water (Figure 13). Interestingly, this dependence shows no similarity to the dependence of the diffusion coefficient on water content (Figure 2). It is therefore unlikely that the mechanism of proton migration from the OH group to the quenching site(s) resembles that of proton mobility.

The observation of Shizuka,<sup>32</sup> that the hydroxy group plays a major role in the quenching process, and our observation (Figure 13) of constant  $k_q/k_a$  ratio over most of the concentration range, could be explained if both processes share the same precursor CIP. This could be, for example, the pentameric ring<sup>59,65</sup> bridging the  $O^-$ , via two water molecules, with  $H_5O_2^+$ . Thus, the diffusing proton is attracted predominantly to the  $O^-$  site, where the CIP is formed. This intermediate subsequently leads to either of the two recombination products.

The branching ratio between the two recombination pathways is constant as long as there exist hydrogen-bonded water molecule pathways connecting the CIP with the quenching site(s), suggesting preferential quenching of the 5CN2OH anion through water chains.<sup>66</sup> Only near pure methanol are water molecules solvating the  $O^-$  replaced by methanol and the quenching path is eliminated.

**G. Solvent-Dependent  $R^*O^-$  Deactivation.** It has been shown earlier<sup>67</sup> that the lifetime of the 1-naphtholate anion in alcohol/water and acetonitrile/water mixtures has a bell-shaped dependence on water concentration and reaches a maximum around 50 mol %  $H_2O$ . In the present work a similar dependence was observed for  $\tau_0'$  of 5CN2OH in methanol/water mixtures (Tables 1 and 2, Figure 14). To investigate the effect of water concentration on the 5CN2O<sup>-</sup> lifetime, we separated the rate constants of fluorescence ( $k_f'$ ) and the nonradiative decay ( $k_{nr}'$ ) using the expressions

$$1/\tau_0' = k_f' + k_{nr}' \quad (23)$$

$$\varphi_0' = k_f'\tau_0' \quad (24)$$

where  $\varphi_0'$  is the absolute quantum yield of the anion fluorescence measured here under direct excitation conditions, i.e., at  $pH > pK_a$ , monitored by absorbance spectra (Table 4).

We find that  $k_f'$  is practically solvent-independent (average value ca. 0.02 1/ns). This is in good agreement with the generally recognized theory: The pure radiative rate constant depends

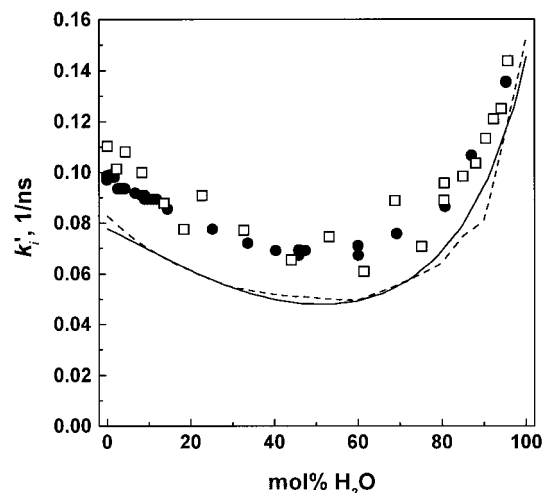


**Figure 14.** Dependence of  $R^*O^-$  deactivation rates on solvent composition. Circles, fluorescence decay rate  $k_f'$ ; squares, inverse fluorescent quantum yield of directly excited naphtholate multiplied by  $k_f' = 0.02$ ; full line is the nonradiative rate constant  $k_{nr}'$ ; dashed line is the linear combination of water/mixture viscosity ratio and reciprocal Debye relaxation time of mixtures. See text for details.

**TABLE 4: Absolute Quantum Yields of  $R^*O^-$  Fluorescence under Direct Excitation in Basic Methanol/Water Mixtures ( $pH > pK_a$ )**

mol % $H_2O$	$\varphi_0'$	mol % $H_2O$	$\varphi_0'$
0	0.181	68.8	0.225
2.2	0.197	75.1	0.283
4.3	0.185	80.4	0.225
8.3	0.200	80.5	0.209
13.6	0.228	85.0	0.203
18.4	0.258	88.0	0.193
22.6	0.220	90.3	0.177
32.6	0.259	92.3	0.165
44.0	0.306	94.1	0.160
53.0	0.269	95.7	0.139
61.4	0.329		

only on the emission wavenumber,<sup>68</sup> which is practically constant for  $R^*O^-$  at any water concentration. The experimental values of  $1/\tau_0'$  are shown in Figure 14 as circles. According to eq 24, the values of  $k_f'/\varphi_0'$  should coincide with the independently measured  $1/\tau_0'$ . One can see in Figure 14 that the dependences of  $0.02/\varphi_0'$  (squares) and  $1/\tau_0'$  (circles) on water content are identical within experimental error. We fitted the data of  $1/\tau_0'$  (or  $0.02/\varphi_0'$ ) to a third-order polynomial:  $1/\tau_0'(x) = 0.097 - 5.2 \times 10^{-4}x - 1.4 \times 10^{-5}x^2 + 2.5 \times 10^{-7}x^3$  1/ns. By subtracting  $k_f' = 0.02$  1/ns, the dependence of  $k_{nr}'$  on solvent composition is obtained as the full curve in Figure 14. Hence, the nonlinear dependencies of  $1/\varphi_0'$  and  $k_0'$  on mol %  $H_2O$  result mainly from the behavior of the nonradiative rate constant.

We tried to correlate the solvent-dependence of  $k_{nr}'$  with known solvent properties, such as viscosity,  $\eta$ , and the Debye relaxation time,  $\tau_D$ . The dependence of  $\eta_{H_2O}/\eta$  has a pronounced minimum at 70 mol % water<sup>40</sup> while  $1/\tau_D$  decreases monotonically from pure water to methanol.<sup>69</sup> Their linear combination fits the bell-shaped dependence of  $k_{nr}'$  on solvent composition according to  $k_{nr}' = 0.04(0.023/\tau_D + \eta_{H_2O}/\eta)$  1/ns (dashed line in Figure 14). Thus the bell-shaped dependence of  $k_{nr}'$  follows that of  $\eta_{H_2O}/\eta$ . So, we assume that  $\tau_D$  and  $\eta$  are sufficient to explain the solvent dependence of  $k_{nr}'$ .

Lee and Robinson observed<sup>70</sup> an analogous bell-shaped dependence for the overall rate constant of 2-anilinonaphthalene (2AN) fluorescence decay in methanol–water mixtures and

attributed it to electron photoejection in the water-rich region and radiationless deactivation in the less polar region. Yuan and Brown<sup>71</sup> observed an increase of the nonradiative decay of aminonaphthalimide derivatives in the water-rich region of ethanol/water mixtures. Alternatively to the electron photoejection mechanism, they suggested that the excitation energy of naphthalimide is dissipated into the stretching modes of a cluster of seven to eight water molecules.

## VI. Conclusions

We have studied excited-state proton transfer from an ultrafast photoacid, 5-cyano-2-naphthol. The range of solvents, investigated in part 1 of this series,<sup>29</sup> is extended to methanol/water mixtures. The enhanced photoacidity of this recently synthesized molecule allows proton transfer to pure methanol. Therefore we could probe the behavior of mixtures in the methanol-rich region, previously inaccessible using conventional photoacids. On the other hand, in water this molecule exhibits some solubility/aggregation problems, which could be solved by synthesizing charged analogues such as cyanonaphtholsulfonates. Work in this direction is in progress.

Several interesting observations emerge from this study. We find that the reaction obeys the mechanism of geminate diffusion control over the whole composition range, and not only in the water-rich region accessible for most photoacids. In this mechanism, the dissociated proton which diffuses in the vicinity of the anion may recombine with it adiabatically, giving rise to a  $t^{-3/2}$  tail in the photoacid fluorescence signal. Cyanonaphthols also undergo nonadiabatic protonation, which quenches the excited singlet and competes with the reversible protonation of the hydroxide moiety. Interestingly, this gives rise to a  $t^{-1/2}$  decay in the conjugated base fluorescence.<sup>55</sup>

Fortunately, the theory for these competing diffusion-influenced reactions in the excited state has recently been developed,<sup>34,35</sup> and it produced the dual power law observed experimentally. The present study reports a unique agreement with this theory. Our data, over more than 2 orders of magnitude in time and 3 orders of magnitude in intensity, fits the theory in which only the three rate parameters were adjusted. Moreover, the same parameters explain simultaneously the behavior of both acid and base. In comparison, kinetic rate theory with three rate parameters would not explain the behavior of even one of the two species, because it necessarily leads to exponential, rather than power law, asymptotics. Thus diffusion theory is indispensable in treating fast liquid-phase reactions.

The good agreement between experiment and theory lends credit to the derived dependence of the three rate parameters on solvent composition. First, we have considered the dissociation rate parameter,  $k_d$ . As water is added to methanol, the driving force to the reaction increases and dissociation proceeds faster. The concomitant decrease of the  $pK_a^*$  value with increasing water content is dominated by enhanced proton (and contact ion pair, CIP) stabilization near pure methanol and diminishing anion stabilization in the water-rich region.<sup>9</sup> A structure–reactivity correlation between  $k_d$  and  $pK_a^*$ , over the whole composition range, showed only small deviations from linearity, which could be attributed to the varying dielectric constant. Thus this reaction is still in the endothermic regime. Yet stronger photoacids are required to reach the ultimate dissociation rate in proton transfer to solvent.

An interesting dependence of  $k_d$  on water concentration was revealed. When data from various photoacids was compared, we found a nearly quadratic dependence for the “ordinary” photoacids, such as hydroxypyrenetrisulfonate, which changed

to a linear (or sublinear) dependence for cyanonaphthols. Possibly a requirement for having a  $H_5O_2^+$  moiety in the CIP is relaxed with enhanced photoacidity. In “super” photoacids, the driving force for dissociation is sufficiently large so the system need not wait for the most favorable water conformation to evolve.

Finally, the ratio of adiabatic and nonadiabatic (quenching) rate parameters appeared constant over most of the composition range, except near pure methanol where the quenching pathway becomes much less probable. Possibly, both paths share the same intermediate CIP structure near the hydroxyl moiety. Branching into the quenching route requires at least one intact hydrogen-bonded water molecule pathway connecting the CIP to the quenching site on the distal ring.

**Acknowledgment.** We thank Boiko Cohen for help with data fitting. K.M.S. is supported by a postdoctoral fellowship from The Israeli Council of Higher Education. D.H. acknowledges support from the Israel Science Foundation and the James Franck Program for Laser-Matter Interaction. N.A. acknowledges support from the Israel Science Foundation (129/99-1). The Fritz Haber Research Center is supported by the Minerva Gesellschaft für die Forschung, mbH, München, FRG. L.M.T. acknowledges support by the U.S. National Science Foundation.

## References and Notes

- (1) For reviews see: (a) Weller, A. *Prog. React. Kinet.* **1961**, *1*, 187. (b) Ireland, J. F.; Wyatt, P. A. H. *Adv. Phys. Org. Chem.* **1976**, *12*, 131. (c) Martynov, I. Yu.; Demyashkevich, A. B.; Uzhinov, B. M.; Kuz'min, M. G. *Russ. Chem. Rev.* **1977**, *46*, 1. (d) Arnaut, L. G.; Formosinho, S. J. J. *Photochem. Photobiol. A* **1993**, *75*, 1.
- (2) Trieff, N. M.; Sundheim, B. R. *J. Phys. Chem.* **1965**, *69*, 2044.
- (3) Martynov, I. Yu.; Zaitsev, N. K.; Soboleva, I. V.; Uzhinov, B. M.; Kuz'min, M. G. *J. Appl. Spectrosc.* **1978**, *28*, 732.
- (4) Huppert, D.; Kolodney, E. *Chem. Phys.* **1981**, *63*, 401.
- (5) Lee, J.; Robinson, G. W.; Webb, S. P.; Philips, L. A.; Clark, J. H. *J. Am. Chem. Soc.* **1986**, *108*, 6538.
- (6) Robinson, G. W.; Thistlethwaite, P. J.; Lee, J. *J. Phys. Chem.* **1986**, *90*, 4224.
- (7) Lee, J.; Griffin, R. D.; Robinson, G. W. *J. Chem. Phys.* **1985**, *82*, 4920.
- (8) Masad, A.; Huppert, D. *Chem. Phys. Lett.* **1991**, *180*, 409.
- (9) Agmon, N.; Huppert, D.; Masad, A.; Pines, E. *J. Phys. Chem.* **1991**, *95*, 10407. Erratum *J. Phys. Chem.* **1992**, *96*, 2020.
- (10) Suwaiyan, A.; Al-Adel, F.; Hamdan, A.; Klein, U. K. A. *J. Phys. Chem.* **1990**, *94*, 7423.
- (11) (a) Than Htun, M.; Suwaiyan, A.; Klein, U. K. A. *Chem. Phys. Lett.* **1995**, *243*, 71; (b) *Chem. Phys. Lett.* **1995**, *243*, 506; (c) *Chem. Phys. Lett.* **1995**, *243*, 512; (d) *Chem. Phys. Lett.* **1997**, *264*, 285.
- (12) Das, R.; Mitra, S.; Mukherjee, S. *Chem. Phys. Lett.* **1994**, *221*, 368.
- (13) Schulman, S. G.; Kelly, R. N.; Chen, S. *Chim. Oggi* **1990**, *8*, 13.
- (14) Fillingim, T. G.; Luo, N.; Lee, J.; Robinson, G. W. *J. Phys. Chem.* **1990**, *94*, 6368.
- (15) Schulman, S. G.; Townsend, R. W.; Baeyens, W. R. G. *Anal. Chim. Acta* **1995**, *303*, 25.
- (16) Tolbert, L. M.; Harvey, L. C.; Lum, R. C. *J. Phys. Chem.* **1993**, *97*, 13335.
- (17) Pines, E.; Fleming, G. R. *J. Phys. Chem.* **1991**, *95*, 10448.
- (18) Pines, E.; Pines, D.; Barak, T.; Magnes, B.-Z.; Tolbert, L. M.; Haubrich, J. E. *Ber. Bunsen-Ges. Phys. Chem.* **1998**, *102*, 511.
- (19) Schulman, S. G.; Kelly, R. N.; Gonzalez, J. *Pure Appl. Chem.* **1987**, *59*, 655.
- (20) Mitra, S.; Das, R.; Guha, D.; Mukherjee, S. *Spectrochim. Acta A* **1998**, *54*, 1073.
- (21) (a) Pines, E.; Huppert, D.; Agmon, N. *J. Chem. Phys.* **1988**, *88*, 5620. (b) Agmon, N.; Pines, E.; Huppert, D. *J. Chem. Phys.* **1988**, *88*, 5631.
- (22) (a) Zaitsev, N. K.; Demyashkevich, A. B.; Kuz'min, M. G. *High Energy Chem.* **1979**, *13*, 288. (b) Gutman, M.; Nachliel, E. *Biochim. Biophys. Acta* **1990**, *1015*, 391.
- (23) *Solute–Solvent Interactions*; Coetzee, J. F., Ritchie, C. D., Eds.; Marcel Dekker: New York, London, 1978.
- (24) Bosch, E.; Bou, P.; Allemann, H.; Rosés, M. *Anal. Chem.* **1996**, *68*, 3651.



- (25) *Correlation Analysis in Chemistry*; Chapman, N. B., Shorter, J., Eds.; Plenum Press: New York, London, 1978.
- (26) (a) Tolbert, L. M.; Haubrich, J. E. *J. Am. Chem. Soc.* **1990**, *112*, 8163; (b) *J. Am. Chem. Soc.* **1994**, *116*, 10593.
- (27) Carmeli, I.; Huppert, D.; Tolbert, L. M.; Haubrich, J. E. *Chem. Phys. Lett.* **1996**, *260*, 109.
- (28) Huppert, D.; Tolbert, L. M.; Linares-Samaniego, S. *J. Phys. Chem. A* **1997**, *101*, 4602.
- (29) Solntsev, K. M.; Huppert, D.; Agmon, N. *J. Phys. Chem. A* **1999**, *103*, 6984.
- (30) See, for example: Allinger, N. L.; Cava, M. P.; et al. *Organic Chemistry*; Worth Publishers: New York, 1974.
- (31) Rosenberg, J. L.; Brinn, I. *J. Phys. Chem.* **1972**, *76*, 3558.
- (32) Shizuka, H. *Acc. Chem. Res.* **1985**, *18*, 141.
- (33) Webb, S. P.; Phillips, L. A.; Yeh, S. W.; Tolbert, L. M.; Clark, J. H. *J. Phys. Chem.* **1986**, *90*, 5154.
- (34) Gopich, I. V.; Solntsev, K. M.; Agmon, N. *J. Chem. Phys.* **1999**, *110*, 2164.
- (35) Agmon, N. *J. Chem. Phys.* **1999**, *110*, 2175.
- (36) Solntsev, K. M.; Agmon, N. *Chem. Phys. Lett.* **2000**, *320*, 262.
- (37) Krissinel', E. B.; Agmon, N. *J. Comput. Chem.* **1996**, *17*, 1085.
- (38) Eigen, M. *Angew. Chem., Int. Ed. Engl.* **1964**, *3*, 1.
- (39) Bates, R. G.; Robinson, R. A. In *Chemical Physics of Ionic Solutions*; Conway, B. E., Barradas, R. G., Eds.; John Wiley: New York, 1966.
- (40) Timmermans, J. *Physico-Chemical Constants of Binary Mixtures*; Interscience: New York, 1960; Vol. 4.
- (41) Mashimo, S.; Kuwabara, S.; Yagihara, S.; Higasi, K. *J. Chem. Phys.* **1989**, *90*, 3292.
- (42) Akhadvov, Y. Y. *Dielectric Properties of Binary Solutions*; Pergamon Press: Oxford, New York, 1981.
- (43) *Water. A Comprehensive Treatise*; Franks, F., Ed.; Plenum Press: New York, London, 1972; Vol. 1.
- (44) Erdey-Grúz, T. *Transport Phenomena in Aqueous Solutions*; A. Hilger: London, 1974.
- (45) Erdey-Grúz, T.; Kugler, E.; Majthényi, L. *Electrochim. Acta* **1968**, *13*, 947.
- (46) Weller, A. Z. *Phys. Chem. (München)* **1958**, *17*, 224.
- (47) Lawrence, M.; Marzzacco, C. J.; Morton, C.; Schwab, C.; Halpern, A. M. *J. Phys. Chem.* **1991**, *95*, 10294.
- (48) Sherwood, T. K.; Pigford, R. L.; Wilke, C. R. *Mass Transfer*; McGraw-Hill: New York, 1975.
- (49) (a) Sharma, L. R.; Kalia, R. K. *J. Chem. Eng. Data* **1977**, *22*, 39. (b) Gerhardt, G.; Adams, R. N. *Anal. Chem.* **1982**, *54*, 2618.
- (50) *Handbook of Chemistry and Physics*, 61st ed.; Weast, R. C., Astle, M. J., Eds.; CRC Press: Boca Raton, FL, 1981.
- (51) Shirota, H.; Pal, H.; Tominaga, K.; Yoshihara, K. *J. Phys. Chem.* **1996**, *100*, 14575.
- (52) Chen, Y.; Gai, F.; Petrich, J. W. *Chem. Phys. Lett.* **1994**, *222*, 329.
- (53) Bardez, E. *Isr. J. Chem.* **1999**, *39*, 319.
- (54) Solntsev, K. M.; Huppert, D.; Tolbert, L. M.; Agmon, N. *J. Am. Chem. Soc.* **1998**, *120*, 7981.
- (55) (a) Pines, E.; Fleming, G. R. *Chem. Phys.* **1994**, *183*, 393. (b) Pines, E.; Tepper, D.; Magnes, B.-Z.; Pines, D.; Barak, T. *Ber. Bunsen-Ges. Phys. Chem.* **1998**, *102*, 504.
- (56) Pines, E.; Magnes, B.-Z.; Lang, M. J.; Fleming, G. R. *Chem. Phys. Lett.* **1997**, *281*, 413.
- (57) Marcus, R. A. *J. Phys. Chem.* **1968**, *72*, 891.
- (58) (a) Agmon, N.; Levine, R. D. *Chem. Phys. Lett.* **1977**, *52*, 197. (b) *Isr. J. Chem.* **1980**, *19*, 330.
- (59) Agmon, N. *J. Phys. Chem. A* **1998**, *102*, 192.
- (60) Huppert, D. Unpublished data.
- (61) (a) Ando, K.; Hynes, J. T. *J. Mol. Liq.* **1995**, *64*, 25. (b) *J. Phys. Chem. B* **1997**, *101*, 10464.
- (62) (a) Ivanov, V. L.; Martynov, I. Yu.; Uzhinov, B. M.; Kuz'min, M. G. *High Energy Chem.* **1977**, *11*, 361. (b) Zaitsev, N. K.; Demyashkevich, A. B.; Kuz'min, M. G. *High Energy Chem.* **1978**, *12*, 361. (c) Shapovalov, V. L.; Demyashkevich, A. B.; Kuz'min, M. G. *Sov. J. Chem. Phys.* **1985**, *2*, 884.
- (63) (a) Harris, C. M.; Selinger, B. K. *J. Phys. Chem.* **1980**, *84*, 891; (b) *J. Phys. Chem.* **1980**, *84*, 1366.
- (64) Lee, J.; Robinson, G. W.; Bassez, M.-P. *J. Am. Chem. Soc.* **1986**, *108*, 7477.
- (65) Agmon, N. *J. Mol. Liq.* **2000**, *85*, 87.
- (66) As was mentioned in section V.A, spectroscopically we find evidence for preferential solvation in acetonitrile/water, but not in MeOH/H<sub>2</sub>O mixtures.
- (67) Webb, S. P. *Picosecond Studies of Excited-State Proton Transfer*. Ph.D. Thesis, UC Berkeley, 1985.
- (68) Birks, J. B. *Photophysics of Aromatic Molecules*; Wiley-Interscience: London, 1970.
- (69) Mashimo, S.; Umehara, T.; Redlin, H. *J. Chem. Phys.* **1991**, *95*, 6257.
- (70) Lee, J.; Robinson, G. W. *J. Am. Chem. Soc.* **1985**, *107*, 6153.
- (71) Yuan, D. W.; Brown, R. G. *J. Phys. Chem. A* **1997**, *101*, 3461.